

Compact instrument for fluorescence image-guided surgery

Xinghua Wang, Srabani Bhaumik, Qing Li, V. Paul Staudinger, and Siavash Yazdanfar

GE Global Research, 1 Research Circle, Niskayuna, New York 12309.

Abstract. Fluorescence image-guided surgery (FIGS) is an emerging technique in oncology, neurology, and cardiology. To adapt intraoperative imaging for various surgical applications, increasingly flexible and compact FIGS instruments are necessary. We present a compact, portable FIGS system and demonstrate its use in cardiovascular mapping in a preclinical model of myocardial ischemia. Our system uses fiber optic delivery of laser diode excitation, custom optics with high collection efficiency, and compact consumer-grade cameras as a low-cost and compact alternative to open surgical FIGS systems. Dramatic size and weight reduction increases flexibility and access, and allows for handheld use or unobtrusive positioning over the surgical field. © 2010 Society of Photo-Optical Instrumentation Engineers. [DOI: 10.1117/1.3378128]

Keywords: fluorescence imaging; image-guided surgery; near infrared.

Paper 09480LRR received Oct. 30, 2009; revised manuscript received Feb. 10, 2010; accepted for publication Mar. 9, 2010; published online Apr. 12, 2010.

Fluorescence imaging is increasingly being employed for surgical guidance, used to minimize iatrogenic damage, expedite surgical procedures, and enhance surgical efficiency, with utility in various clinical fields.¹⁻³ Applications of fluorescence image-guided surgery (FIGS) include sentinel lymph node mapping,^{2,3} assessing coronary artery bypass graft patency,⁴ identifying tumors intraoperatively,^{5,6} and minimizing the risk of iatrogenic bile duct injury.⁷ Many of these applications, such as imaging of lymphatics or vasculature, are enabled by nontargeted fluorescent contrast agents such as indocyanine green or methylene blue (MB).

Contrast agents emitting in the NIR region of the optical spectrum (700 to 1000 nm) provide several advantages over agents in the visible region.⁸ Tissue constituents that dominate absorption of light in the visible have absorption minima in the red to NIR. Moreover, there is a dramatic decrease in scattering in the NIR relative to visible wavelengths. The reduced absorption and scattering results in less light attenuation and thus deeper penetration. Imaging in the NIR also minimizes background, as most endogenous fluorescent species emit in the visible spectrum.⁹ In FIGS, one channel typically images the fluorescence emission, while the other channel simultaneously captures a color video of the surgical area. Thus, emission in the NIR also allows for minimal spectral overlap between the color and fluorescence channels, result-

ing in higher color fidelity and higher fluorescence collection efficiency. FIGS instrumentation has been developed for both open and minimally invasive surgeries.²⁻⁷ Several of these instruments feature only a single (fluorescence) channel,^{2,4,6,7} or have a relatively large footprint.²⁻⁴ To improve access and increase the clinical utility of FIGS, particularly for open surgical applications,³ the size of existing imaging systems has to be reduced for greater flexibility and mobility. Here we describe the development of a compact dual-mode imaging probe and demonstrate its use in cardiovascular surgery in a preclinical model.

Our strategy for size reduction addresses illumination, detection, and optics. First, the system uses fiber optic delivery of both excitation and illumination. Conventional systems often house the light source, potentially including electronics and active cooling, in the image head.^{2,6,10} By displacing the light sources from the imaging head to a medical cart, we have eliminated the weight of the sources and thermal management. Second, we have replaced the imaging cameras with compact "lipstick" cameras. Prevalent in consumer electronics and security applications, these cameras are affordable, lightweight (~25 g.) and readily available for integration. In comparison to the substantially larger, high gain (e.g., intensified²) or actively cooled, scientific grade³ cameras often used in FIGS, consumer-grade lipstick cameras are less sensitive. For example, lipstick cameras have smaller active detector areas and/or smaller pixels, resulting in lower sensitivity. Thus, our third strategy to maintain compactness without compromising sensitivity was a custom optical design with high collection efficiency.

The compact instrument [Fig. 1(a)] was designed for use with MB, a dye with a wide range of clinical utility approved by the United States Food and Drug Administration. While it is commonly used as a stain with deep blue hue, MB is also a fluorophore in the NIR, emitting around 700 nm.^{3,11} Excitation light was provided by a monochromatic 500-mW (class 3b), 660-nm laser diode (PLT Technology PLT-660, Santa Barbara, California) delivered to the imaging head through an excitation clean-up filter (Semrock FF01-655/40, Rochester, New York) and a 2-mm plastic fiber (Timbercon CA-005-255-255-001M-197, Lake Oswego, Oregon). Approximately 300 mW of excitation power emerged from the fiber distal end, corresponding to ~60% coupling efficiency. A 4.6-W white LED (Vision Light Tech HSL-58SW-D300, Uden, The Netherlands) provided white light illumination through a second delivery fiber. A 15-mm focal length aspherical lens (Thorlabs AL1815-A, Newton, New Jersey) was used to generate a top-hat uniform illumination at a working distance of 75 to 300 mm. Fluorescence emission from the sample was collected through a dichroic mirror (Semrock FF677-Di01), an emission filter (Semrock FF01-716/40), and a custom designed and fabricated fixed-focus Cooke triplet (Table 1), designed to operate from 450 to 1000 nm. The entrance pupil diameter (EPD) of this lens is large (~7 mm) compared to the off-the-shelf optics (~3 mm, Watec Cameras, Orangeburg, New York) used on the white light channel, translating to roughly five times higher collection efficiency. The white light (color) and fluorescence (monochrome) channels each have a dedicated, lipstick charge-coupled device camera (Wa-

Address all correspondence to: Siavash Yazdanfar, GE Global Research, 1 Research Circle, KW C287, Niskayuna, New York 12309. Tel: 518-387-4492; Fax: 518-387-7021; E-mail: siavash.yazdanfar@research.ge.com

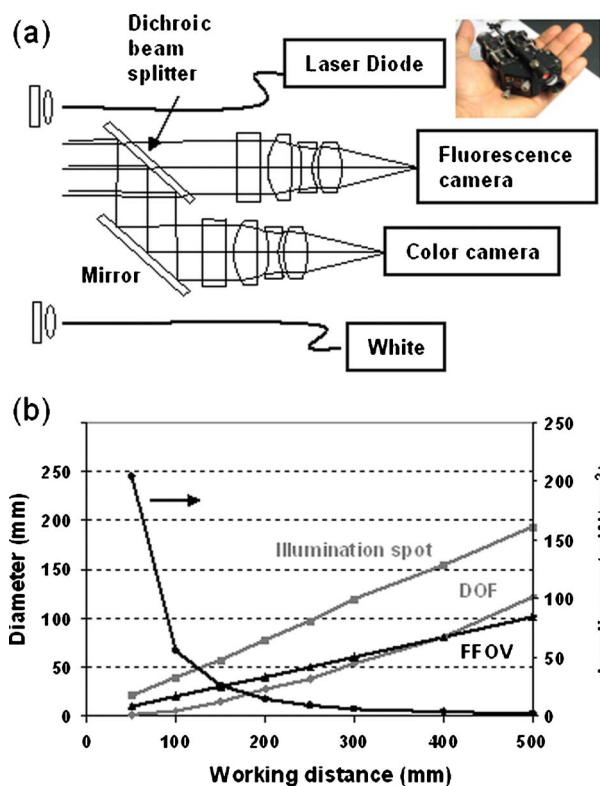


Fig. 1 (a) Schematic diagram and picture (inset) of compact FIGS instrument. (b) Performance of the FIGS hand-held system as a function of working distance. DOF is depth of field, and FFOV is the full field of view.

Table 1 Detailed design parameters of a custom Cooke triplet, designed with image side $f/\text{number}=1.8$, effective focal length = 14.5 mm, full field of view = 16 deg, and distortion < 1%. R is radius, T is thickness, and Inf is infinity.

Surface	R (mm)	T (mm)	Glass	Semi aperture
Object	Inf	300.0		
1	Inf	3.500	458.678	4.14
2	Inf	1.000		4.07
3	7.8475	2.490	SLAM2_OHARA	4.02
4	-63.4134	0.900		3.70
5	-18.2233	3.000	STIH4_OHARA	3.31
6	5.4532	0.971		2.61
Stop	Inf	0.800		2.65
8	10.2720	4.600	SLAM2_OHARA	3.01
9	-12.0082	3.000		3.17
10	Inf	5.636		2.72
Image	Inf	0.482		1.93

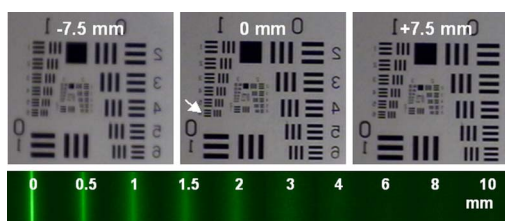


Fig. 2 Top: through focus white light images of a USAF 1951 resolution target, optimized at a 150-mm working distance. The arrow corresponds to 3.56 lp/mm. Bottom: images of 1- μM methylene blue fluorescence from a 1.5-mm diameter tube under increasing depths of 1% Intralipid.

tec 240 and 704R, respectively). The analog outputs of both cameras were digitized at 30 frames per second using a dual channel framegrabber (Matrox Morphis MOR/2VD, Dorval, Quebec) and displayed using custom image acquisition software developed in C++ and Matrox MIL-8.0. Video streams from both channels were recorded uncompressed in AVI format to a RAID disk array in real time. Collectively, the imaging head weighed less than 0.5 kg, with a total volume of approximately $65 \times 40 \times 40 \text{ mm}^3$. The total instrument cost was $\sim \$15,000$, roughly the cost of scientific-grade charge-coupled device (CCD)³ or intensified cameras² used in other FIGS instruments.

Theoretical performance parameters of the hand-held probe are shown as a function of working distance (WD) in Fig. 1(b). Irradiance at the sample drops geometrically with distance, while the illumination spot diameter, depth of field (DOF), and imaging full field of view (FFOV) increase linearly with WD. Using the laser diode excitation source, the irradiance at the sample can provide adequate excitation power density ($> 5 \text{ mW/cm}^2$) at up to $\sim 300 \text{ mm}$ WD. Optimized for a typical WD of 150 mm, the DOF is $\sim 15 \text{ mm}$, defined by the location where the modulation transfer function (MTF) drops by 15% relative to best focus. While 15 mm seems somewhat limited, a low DOF is a consequence of increasing the EPD. Furthermore, the image quality can be acceptable over a wider range, as a 15% drop in the MTF is quite stringent and maintains images with fairly high image quality (Fig. 2). An MTF of > 0.6 is achieved at 50 line pairs per mm (lp/mm) at the image plane, corresponding to a sharp image quality and a high spatial resolution of 5 lp/mm ($100 \mu\text{m}$) at the object plane. Sensitivity of the fluorescence channel is also shown in Fig. 2 by collecting images of 1- μM MB in a 1.5-mm-diam glass tube as a function of depth in 1% Intralipid. The geometry of the sample is consistent with that of a tubular structure such as the ureter, and the concentration of the dye is acceptable for clinical use.³

Following design and construction of the hand-held imaging device, we performed preclinical FIGS for an application in cardiovascular stem cell therapy. Implantation of stem cells to regenerate cardiomyocytes is an emerging technique for restoring heart function. Differentiation of stem cells into viable cardiomyocytes may vary depending on the injection site, preferably within the infarct or peri-infarct zone adjacent to healthy myocardium.¹² Thus a precise way to visualize this border zone along with healthy vasculature, i.e., tissue premapping, may be critical for efficacy of cardiovascular stem cell therapy.

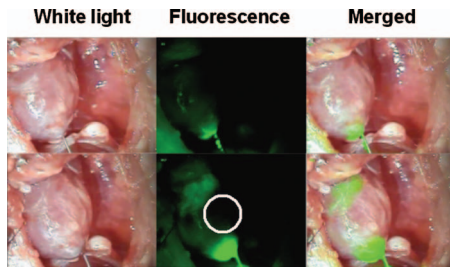


Fig. 3 Preclinical image-guided surgery for vasculature mapping in a rat heart at time of injection (top) and shortly (~60 s) after injection (bottom). The fluorescence channel clearly indicates ischemic regions of the heart, approximated by the circle, which are otherwise inconspicuous in the white light channel. The field of view is approximately $25 \times 25 \text{ mm}^2$.

Animal experiments were performed in accordance with a protocol approved by the Institutional Animal Care and Use Committee at GE Global Research. We applied a well-established murine model of myocardial infarction that has been employed to examine the efficacy of therapeutic interventions on cardiac remodeling and survival.¹³ Briefly, the left anterior descending coronary artery in a male Wistar Hannover rat was ligated to induce an ischemic infarct in the free wall of the left ventricle. Over time, the infarct area is replaced by fibrotic tissue, and adjacent cardiac tissue becomes hypertrophic. Five months later, a second operation was performed to identify the viable regions of the heart, free of ischemia and fibrosis. The compact probe was mounted over the surgical field for hands-free operation at a working distance of ~150 mm. A 50- μL bolus of MB with 70- μM concentration was injected into the left ventricle to highlight the vasculature in the healthy tissue. Whereas Fig. 2 demonstrated the high sensitivity of the imaging system, a higher dose was used for *in vivo* imaging, to increase signal levels while avoiding an adverse response to MB. The injected bolus dose of 70 μM (corresponding to ~4 $\mu\text{g}/\text{kg}$) was ~500-fold lower than previous pharmacokinetics studies of MB.¹⁴

Due to the circulation of the fluorophore in the vasculature and its uptake by healthy tissue, fluorescence serves to provide negative contrast to the scar region, which was not visible under white light. The still images (Fig. 3) extracted from real-time (30 fps) recorded video demonstrate high color fidelity and sharp focus. The addition of a fluorescence modality improves real-time intraoperative visualization of critical structures, in this case the precise location of potentially ischemic tissue resulting from the infarct. Additionally, the compact image head design allowed for rapid and flexible repositioning during surgery.

In summary, we have developed a compact instrument for FIGS and demonstrated its use in a preclinical model. The system uses fiber optic delivery of laser diode excitation, along with a custom optical design with high collection efficiency and compact consumer-grade cameras, to minimize the volume and weight. While the current hand-held probe is designed for use with MB, it can easily be adapted for use with other contrast agents simply by replacing the excitation light

source and filters. Dramatic size reduction increases flexibility and access, and allows for portable use or unobtrusive mounting over the surgical field. This instrument is complementary to other small form factor devices developed primarily for spectroscopic and tomographic applications.¹⁵

Acknowledgments

We appreciate helpful discussions with Chris Unger, Cynthia Davis, and Pavel Fomitchov.

References

1. W. Stummer, U. Pichlmeier, T. Meinel, O. D. Wiestler, F. Zanella, and H.-J. Reulen, "Fluorescence-guided surgery with 5-aminolevulinic acid for resection of malignant glioma: a randomised controlled multicentre phase III trial," *Lancet Oncol.* **7**, 392–401 (2006).
2. E. M. Sevick-Muraca, R. Sharma, J. C. Rasmussen, M. V. Marshall, J. A. Wendt, H. Q. Pham, E. Bonefas, J. P. Houston, L. Sampath, K. E. Adams, D. K. Blanchard, R. E. Fisher, S. B. Chiang, R. Elledge, and M. E. Mawad, "Imaging of lymph flow in breast cancer patients with microdose administration of a near-infrared fluorophore: feasibility study," *Radiology* **246**, 734–741 (2008).
3. S. L. Troyan, V. Kianzad, S. L. Gibbs-Strauss, S. Gioux, A. Matsui, R. Oketokoun, L. Ngo, A. Khamene, F. Azar, and J. V. Frangioni, "The FLARE™ intraoperative near-infrared fluorescence imaging system: A first-in-human clinical trial in breast cancer sentinel lymph node mapping," *Ann. Surg. Oncol.* **16**, 2943–2952 (2009).
4. L. Balacumaraswami and D. P. Taggart, "Intraoperative imaging of techniques to assess coronary artery bypass graft patency," *Ann. Thorac. Surg.* **83**, 2251–2257 (2007).
5. V. X. D. Yang, P. J. Muller, P. Herman, and B. C. Wilson, "A multi-spectral fluorescence imaging system: design and initial clinical tests in intra-operative photofrin-photodynamic therapy of brain tumors," *Lasers Surg. Med.* **32**, 224–232 (2003).
6. T. Ishizawa, N. Fukushima, J. Shibahara, K. Masuda, S. Tamura, T. Aoki, K. Hasegawa, Y. Beck, M. Fukayama, and N. Kokudo, "Real-time identification of liver cancers by using indocyanine green fluorescent imaging," *Cancer* **115**, 2491–2504 (2009).
7. B. M. Stiles, P. S. Adusumilli, A. Bhargava, and Y. Fong, "Fluorescent cholangiography in a mouse model: an innovative method for improved laparoscopic identification of the biliary anatomy," *Surg. Endosc.* **20**, 1291–1295 (2006).
8. J. V. Frangioni, "In vivo near-infrared fluorescence imaging," *Curr. Opin. Chem. Biol.* **7**, 626–634 (2003).
9. R. Richards-Kortum and E. Sevick-Muraca, "Quantitative optical spectroscopy for tissue diagnosis," *Annu. Rev. Phys. Chem.* **47**, 555–606 (1996).
10. S. Gioux, V. Kianzad, R. Ciocan, S. Gupta, R. Oketokoun, and J. V. Frangioni, "High-power, computer-controlled, light-emitting diode-based light sources for fluorescence imaging and image-guided surgery," *Mol. Imaging* **8**, 156–165 (2009).
11. M. Chu and Y. Wan, "Sentinel lymph node mapping using near-infrared fluorescent methylene blue," *J. Biosci. Bioeng.* **107**, 455–459 (2009).
12. H. C. Quevedo, K. E. Hatzistergos, B. N. Oskouei, G. S. Feigenbaum, J. E. Rodriguez, D. Valdes, P. M. Pattany, J. P. Zambrano, Q. H. Hu, I. McNiece, A. W. Heldman, and J. M. Hare, "Allogeneic mesenchymal stem cells restore cardiac function in chronic ischemic cardiomyopathy via trilineage differentiating capacity," *Proc. Natl. Acad. Sci. U.S.A.* **106**, 14022–14027 (2009).
13. J. Wang, H. Bo, X. Meng, Y. Wu, Y. Bao, and Y. Li, "A simple and fast experimental model of myocardial infarction in the mouse," *Tex Heart Inst. J.* **33**, 290–293 (2006).
14. C. Peter, D. Hongwan, A. Küpfer, and B. H. Lauterburg, "Pharmacokinetics and organ distribution of intravenous and oral methylene blue," *Eur. J. Clin. Pharmacol.* **56**, 247–250 (2000).
15. S. J. Erickson and A. Godavarty, "Hand-held based near-infrared optical imaging devices: a review," *Med. Eng. Phys.* **31**, 495–509 (2009).